

1 Design and test performance of the ATLAS Feature 2 Extractor trigger boards for the Phase-1 Upgrade

3 **Weiming Qian***

4 *STFC Rutherford Appleton Laboratory,*
5 *Chilton, Didcot, Oxon, OX11 0QX, United Kingdom*
6 *E-mail: Weiming.Qian@stfc.ac.uk*

7 ABSTRACT: In Run 3, the ATLAS Level-1 Calorimeter Trigger will be augmented by an
8 Electron Feature Extractor (eFEX), to identify isolated e/γ and τ particles, and a Jet Feature
9 Extractor (jFEX), to identify energetic jets and calculate various local energy sums. Each
10 module accommodates more than 450 differential signals that can operate at up to 12.8 Gb/s,
11 some of which are routed over 30 cm between FPGAs. Presented here are the module designs,
12 the processes that have been adopted to meet the challenges associated with multi-Gb/s PCB
13 design, and the results of tests that characterize the performance of these modules.

14 KEYWORDS: Trigger; Feature Extractor; ATCA; PCB simulation.



15	Contents	
16	1. Introduction	1
17	1.1 ATLAS Level-1 Calorimeter Trigger architecture for Phase-I Upgrade	1
18	1.2 Trigger algorithms and performance	2
19	2. Prototype design	3
20	2.1 eFEX	3
21	2.1.1 Processing Area	3
22	2.1.2 eFEX prototype	4
23	2.2 jFEX	4
24	2.2.1 Processing area	4
25	2.2.2 jFEX prototype	5
26	2.3 PCB design method	6
27	3. Prototype test	6
28	3.1 Link speed test results	7
29	3.2 Link speed decision	8
30	4. Conclusion	8
31		
32		
33		

34 1. Introduction

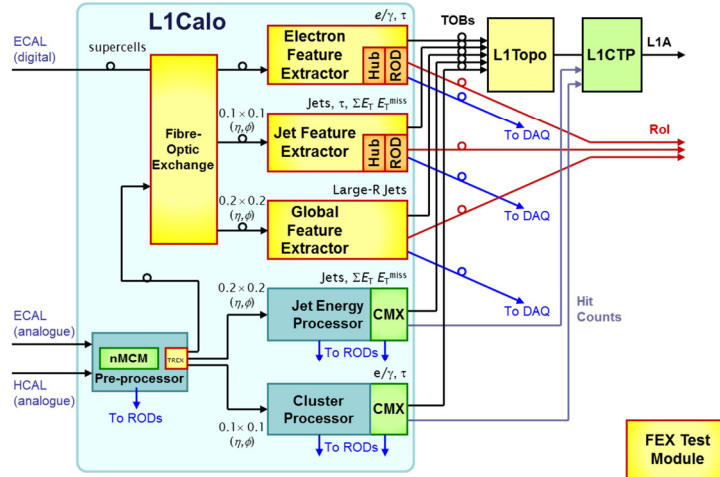
35 In Run 3 (starting in 2021), the LHC [1] luminosity will double (to $\sim 2.5 \times 10^{34} \text{ cm}^{-2} \text{ s}^{-1}$),
36 which will greatly increase the pileup rate. However, the ATLAS [2] front-end detector
37 electronics will remain largely unchanged. Hence the total ATLAS Level-1 Trigger [3] rate will
38 still be limited by the readout bandwidth of the front-end electronics to 100 KHz or less.
39 Moreover, the Level-1 Trigger must retain sensitivity to the physics electroweak processes and
40 stay within the current ATLAS Level-1 latency envelope of $2.5 \mu\text{s}$. To meet these challenges, the
41 Phase-I Upgrade [4] to the ATLAS Level-1 Trigger system is needed.

42 1.1 ATLAS Level-1 Calorimeter Trigger architecture for Phase-I Upgrade

43 Figure 1 shows the architecture of the Phase-I Upgrade of the ATLAS Level-1 Calorimeter
44 Trigger (L1Calo) [5]. The current L1Calo system is augmented by three additional feature-
45 identification subsystems:

- 46 • the electromagnetic Feature Extractor (eFEX), comprising eFEX modules and Hub
47 modules with Readout Driver (ROD) daughter cards, which identifies isolated e/γ and τ
48 candidates, using data of finer granularity than is currently available to L1Calo;
- 49 • the jet Feature Extractor (jFEX), comprising jFEX modules and Hub modules with
50 ROD daughter cards, which identifies energetic jets and computes various local energy

- 51 sums, using data of finer granularity than that available to the current L1Calo JEP
 52 subsystem;
- 53 • the global Feature Extractor (gFEX [6]), comprising one gFEX module, which identifies
 54 calorimeter trigger features requiring the complete calorimeter data.



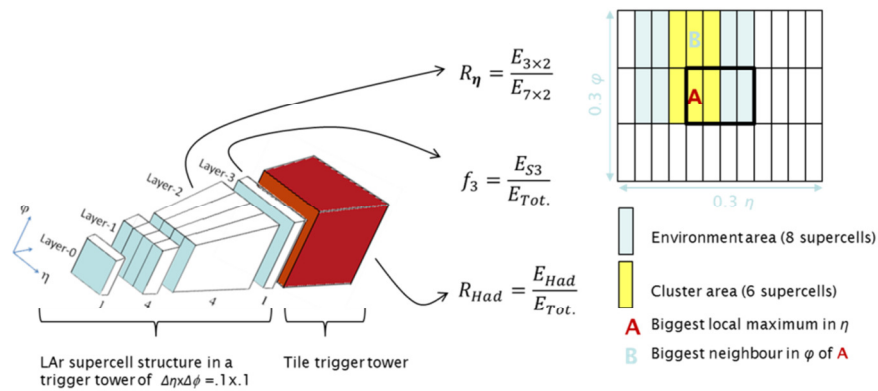
55
56 **Figure 1. ATLAS Level-1 Calorimeter Trigger Phase-I Upgrade [7]**

57 In addition to these, the Phase-I upgrade of L1Calo includes the Tile Rear Extension
 58 (TRES) to the Pre-Processor (PPr) subsystem, which digitizes Tile data and transmits them to
 59 the FEXs optically, the Fibre Optical Exchange (FOX), and the FEX Test Module (FTM),
 60 which facilitates the testing of FEX modules before system-level commissioning.

61 Apart from the small number of PPr modules that digitize Tile data for the FEXs, the
 62 current L1Calo system, comprising the Pre-Processor, Jet Energy Processor (JEP) and Cluster
 63 Processor (CP), will be decommissioned after the Phase-I Upgrade is fully commissioned.

64 1.2 Trigger algorithms and performance

65 In the current L1Calo system, the CP processes data from the calorimeters and identifies
 66 energy deposits characteristic of isolated e/γ and τ particles, using Trigger Towers of typical
 67 granularity of 0.1×0.1 ($\eta \times \phi$). The eFEX performs this same function using higher granularity
 68 data from the Liquid Argon (LAr) electromagnetic calorimeter. For each LAr Trigger Tower,
 69 the eFEX receives data from 10 ‘supercells’ in four layers, as shown in Figure 2.



70
71 **Figure 2. eFEX trigger algorithms [8]**

72 This makes it possible to increase the
 73 discriminatory power of L1Calo by running a
 74 collection of new trigger algorithms, including
 75 R_η , f_3 and R_{Had} , that analyse shower shapes. These
 76 algorithms run in a window of 0.3×0.3 ($\eta \times \phi$)
 77 that slides by 0.1 in both η and ϕ (such that
 78 neighbouring instances of the window overlap).

79 Figure 3 shows the results of a simulation
 80 comparing the performance of the current (Run
 81 2) algorithms with the eFEX (Phase I)
 82 algorithms. It shows the eFEX can reduce the
 83 EM trigger rate by a factor of ~ 3 , or allow the
 84 trigger threshold to be lowered by ~ 7 GeV at the
 85 20 KHz reference point. Further optimization on
 86 eFEX algorithms is under study.

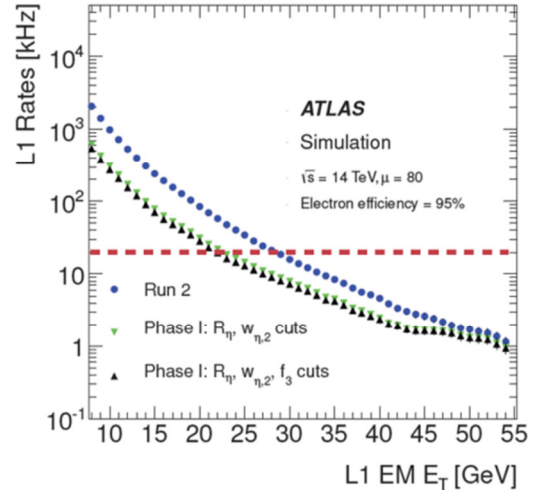


Figure 3. eFEX trigger performance [9]

87 The jFEX identifies jets, and calculates $\sum E_T$ and E_T^{miss} . In the current system, these
 88 functions are implemented by the JEP. The jFEX improves on the performance of the JEP by a
 89 number of means. It receives higher-granularity calorimeter data (0.1×0.1 ($\eta \times \phi$) rather than
 90 0.2×0.2) and implements a Gaussian-weighted filter, giving it greater discriminatory power; it
 91 can implement a larger algorithm window; and each jFEX module processes data from a
 92 complete ring of the calorimeter in ϕ , enabling in-time pileup suppression and improving the
 93 calculation of $\sum E_T$ and E_T^{miss} .

94 Figure 4 shows the results of simulations
 95 comparing the performance of the algorithms that
 96 can be implemented on the jFEX, with those
 97 currently run on the JEP. It shows how the turn-
 98 on curves of the jFEX are sharper – a fact that
 99 can be used to raise the trigger thresholds without
 100 losing efficiency, leading to rate reductions
 101 similar to the eFEX.

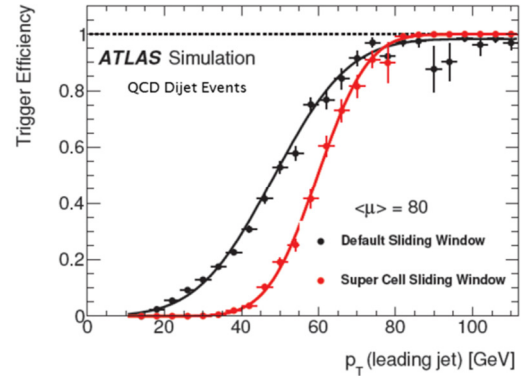


Figure 4. jFEX trigger performance [10]

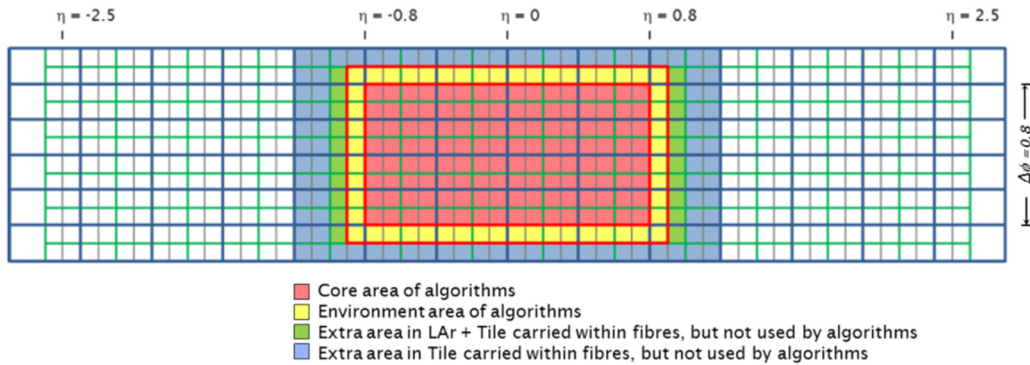
102 2. Prototype design

103 2.1 eFEX

104 2.1.1 Processing Area

105 The eFEX subsystem processes data from the calorimeters within the region of
 106 $2.5 \leq \eta \leq 2.5$ and $0 \leq \phi \leq 2\pi$ — a total volume of ~ 14 Tb/s. Given the limits of current
 107 technology, it is impossible to receive this into a single module. Due to the overlapping nature
 108 of the eFEX algorithm windows, partitioning the subsystem into multiple modules means a
 109 substantial volume of calorimeter data must be duplicated and/or shared between modules (and
 110 between FPGAs on the modules). This partitioning needs to balance the total number of
 111 modules, the number of FPGAs per module, the fibre count per module, the complexity of fibre
 112 mapping between the calorimeters and the eFEX, and the difficulty of sharing data between
 113 adjacent modules and between FPGAs. Figure 5 shows the partitioning of the eFEX prototype
 114 design. The middle eFEX module processes a core calorimeter area of 1.6×0.8 ($\eta \times \phi$), whereas

115 the eFEX modules on two sides process a core calorimeter area of 1.7×0.8 ($\eta \times \phi$). Thus, three
 116 eFEX modules process a complete strip in the η range, and 24 modules are required in total.



117

118

Figure 5. eFEX partitioning [11]

119 2.1.2 eFEX prototype

120 The eFEX prototype, shown in Figure 6, is an
 121 ATCA [12] module with a non-standard physical
 122 form: the front board is extended through Zone 3
 123 into the rear shelf space to optimize the routing of
 124 the input fibres, which are connected to the module
 125 via a custom Rear Transition Module (RTM).

126 The eFEX PCB is a 22-layer board with six
 127 micro-via layers. It houses:

- 128 • 4 Xilinx Virtex-7 [13] FPGAs
- 129 (XC7VX550T) for algorithm processing;
- 130 • 1 Xilinx Virtex-7 FPGA (XCVX330T) for
- 131 control and readout functions;
- 132 • 17 Avago MiniPODs [14] for optical input
- 133 (144 signals) and output (36);
- 134 • 94 high-speed fan-out buffers (NB7VQ14M [15]) for data duplication between FPGAs.

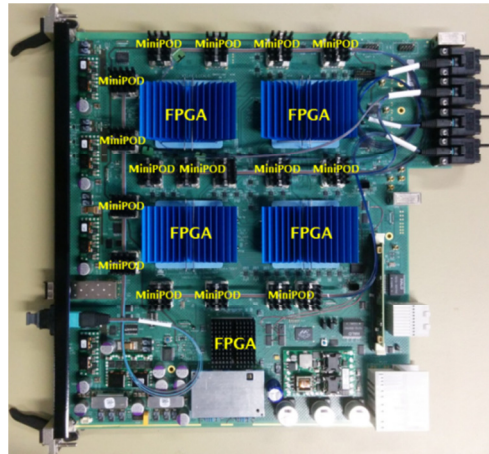


Figure 6. eFEX prototype

135 The high-speed fan-out buffer NB7VQ14M was tested on a previous module, the High-
 136 Speed Demonstrator (HSD) [16]. It exhibited very good signal quality at 10 Gbps with
 137 negligible propagation delay, and hence it was chosen for data duplication on the eFEX.
 138 In total, there are about 450 high-speed multi-Gb/s differential tracks routed on a single eFEX.
 139 Blind and buried vias are used to achieve this density of signal tracks. The PCB is made from a
 140 low loss material (both Isola Itera and Megtron6 have been used on different prototype
 141 modules) and the PCB is rotated by 22° to minimize the effect of PCB fibre glass weave on
 142 differential skew.

143 2.2 jFEX

144 2.2.1 Processing area

145 The jFEX receives data from the calorimeters within the region of $-4.9 \leq \eta \leq 4.9$ and
 146 $0 \leq \phi \leq 2\pi$ — a total volume of $\sim 3\text{Tb/s}$. The jFEX subsystem is partitioned into 7 processing
 147 modules each covering a ϕ ring as shown in Figure 7.

148 This ϕ -ring coverage of each jFEX module enables it to calculate pile-up (i.e. energy
 149 density) for the η range processed, and apply this as a correction to the jet and E_T^{miss} algorithms.

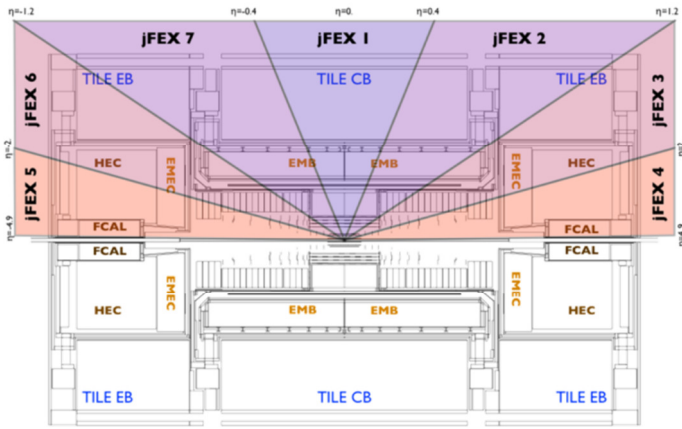


Figure 7. jFEX partitioning

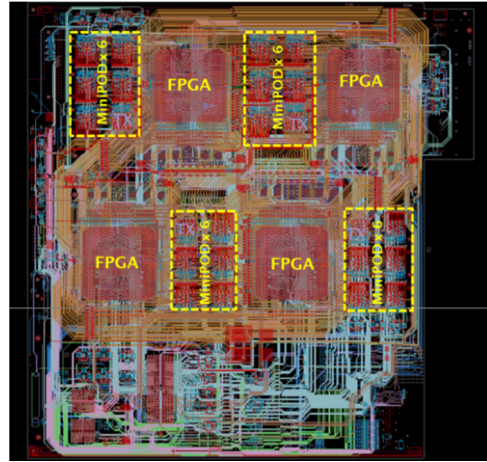


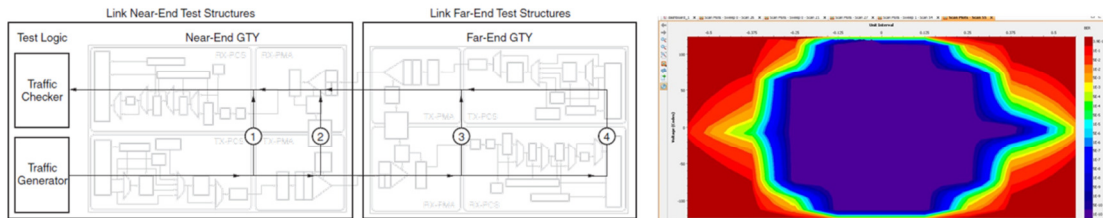
Figure 8. jFEX prototype PCB design

150 **2.2.2 jFEX prototype**

151 The jFEX prototype is currently being manufactured. The PCB layout is shown in Figure
 152 8. It uses the same physical form factor as the eFEX, so that the modules can share the same
 153 RTM design. The jFEX PCB is implemented as a 24-layer board with 8 micro-via layers. It
 154 houses:

- 155 • 4 Xilinx Ultrascale [13] FPGAs (XCVU190) for algorithm processing and readout;
- 156 • 1 mezzanine card for control;
- 157 • 24 Avago MiniPODs for optical input (216 signals) and output (32);

158 Due to its larger algorithm window, the jFEX needs to share even more data between
 159 FPGAs than the eFEX. In total, there are about 540 high-speed multi-Gb/s differential tracks
 160 routed on a single jFEX PCB. A loopback feature of the Xilinx Multi-Gb/s Transceiver (MGT),
 161 Far-End PMA loopback, is used for data-sharing between FPGAs on the jFEX module. This
 162 makes use of the otherwise unused transmitters of MGTs with a small sacrifice of latency.
 163 Figure 9 shows the results of loopback tests done on a Xilinx Evaluation Board VCU110
 164 (Ultrascale XCVU190), which shows a very good eye opening at 25 Gb/s.

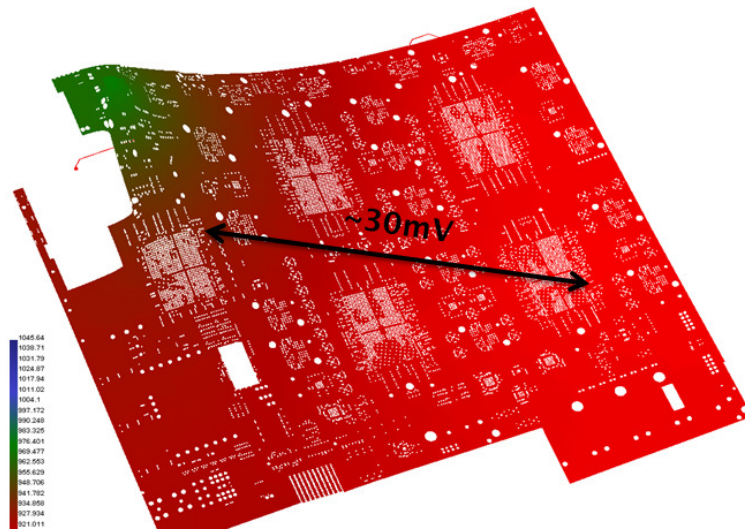


165 **Figure 9. Xilinx MGT Far-End PMA loopback test (path 3 in diagram), IBERT 2-D Eye Scan**
 166 **25Gb/s @ 10^{-11} on Xilinx Evaluation Board VCU110 (Ultrascale XCVU190)**

167

168 **2.3 PCB design method**

169 The eFEX prototype and jFEX prototype share a lot of challenges in PCB design. Firstly, both
170 are very high-density and high-speed PCB boards. The baseline speed of the inputs links
171 specified in the ATLAS Phase-I TDR is 6.4 Gb/s. However, there is always strong desire to run
172 the links faster in order to further improve trigger performance and flexibility. Secondly, both
173 the eFEX and jFEX require complex channel mapping and data sharing. As a consequence,
174 some high-speed links need to run very long signal tracks across the whole PCB between
175 FPGAs. Thirdly, both the eFEX and jFEX have very high power consumption, approaching
176 400W per module. Cooling design will also be very challenging as all the power consumed
177 turns into heat. To meet these challenges, the systematic PCB design method, which was
178 developed with great success in the HSD project, has been adopted in both eFEX and jFEX
179 PCB design. Notably, in addition to signal-integrity simulation, power-integrity simulation (as
180 shown in Figure 10) is particularly important for these modules. The power rails for the FPGA
181 cores and MGTs on both the eFEX and jFEX need to carry more than 100A current; the voltage
182 drops across the power distribution networks thus become significant design constraints.



183
184

Figure 10. eFEX MGT power plane DC voltage drop simulation at 35A

185 **3. Prototype test**

186 After passing initial power-on and boundary scan tests smoothly, the eFEX prototype (Figure 6)
187 was tested with the FTM and the LAr Digital Processing System (DPS) prototype, in a
188 systematic check of all the eFEX high-speed input and output links.

189 In order to validate the TDR baseline link speed and test the upper limit of the possible link
190 speeds, all eFEX high-speed links were tested at three different speeds (6.4 GB/s, 11.2 Gb/s and
191 12.8 Gb/s). The decision on the link speed has a significant impact on the FEX architecture,
192 especially for jFEX, where different link speeds required completely different partitioning.

193 The test setup for these link speed tests is very close to the final system as shown in Figure 1.
194 For example, a FOX demonstrator was used to mimic the complex fibre mapping and insertion
195 loss between the LAr DPS and the eFEX.

196 For the link tests with the LAr DPS, the link sources were Altera Arria 10 FPGAs [17] with
 197 MGTs capable of up to 14 Gb/s. The first eFEX prototype is fitted with Xilinx speed grade -2
 198 Virtex-7 FPGAs, with MGTs specified up to 11.3 Gb/s. The FTM is fitted with a Xilinx speed
 199 grade -3 Virtex-7 FPGAs, with MGTs specified up to 13.1 Gb/s.

200 3.1 Link speed test results

201 The test results obtained for the TDR
 202 baseline link speed of 6.4 Gb/s are
 203 extremely good, with wide-open 2-D eye
 204 scans and Bit Error Rates of less than 10^{-14}
 205 (no error over 3×10^{14} bits) for 257 out
 206 of the 264 input links on the eFEX
 207 prototype.

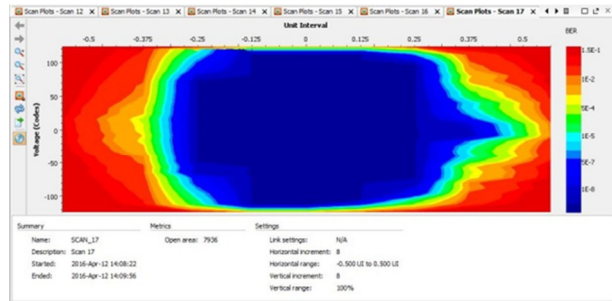


Figure 11. Typical eFEX input link 2-D eye-scan @ 11.2Gb/s

208 At 11.2 Gb/s, the opening of the
 209 2-D eye scans on the eFEX is still very
 210 good, as shown in Figure 11. Figure 12
 211 shows the overall statistics of the open
 212 areas of 2-D eye scans for all eFEX input links at 11.2 Gb/s. The Bit Error Rate on 257 out of
 213 264 eFEX input channels is less than 10^{-14} (no error over 3×10^{14} bits). Of the results for the other
 214 7 links, 4 are correlated to less-optimal PCB routing (which can be improved in next PCB
 215 iteration), and 3 are due to a bad high-speed fan-out buffer (which can be repaired).

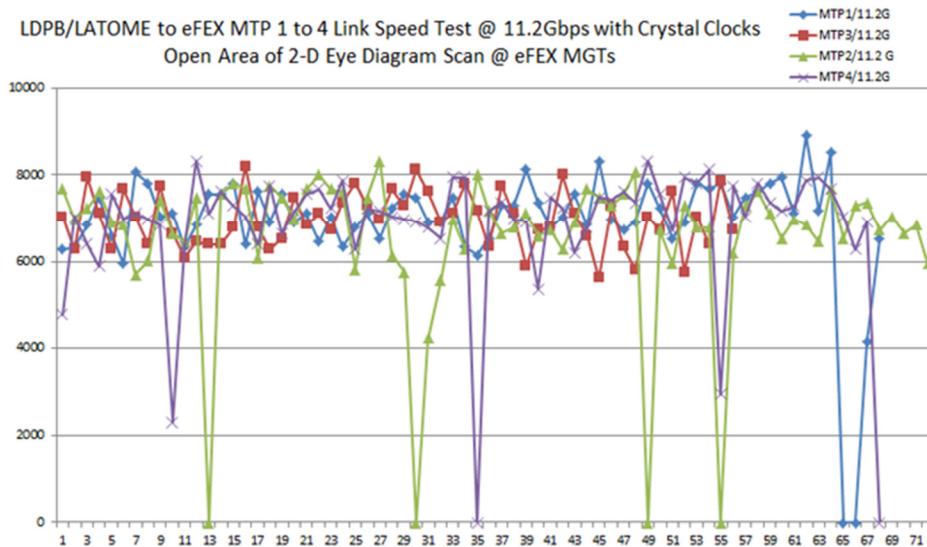


Figure 12. Open Area of 2-D eye scan for all eFEX input links

218 At 12.8 Gb/s, many links on the eFEX prototype still work, but a significant number
 219 fail, as this is outside FPGA MGT's specified speed range. In order to evaluate the eFEX
 220 performance at 12.8 Gb/s, another eFEX prototype will be fitted with Xilinx speed grade -3
 221 Virtex-7 FPGA, with MGTs capable of running up to 13.1 Gb/s.

222 3.2 Link speed decision

223 Based on the above excellent test results, and previous test results between the LAr DPS and the
224 L1Calo gFEX, 11.2 Gb/s has been adopted as the new baseline link speed between LAr and
225 L1Calo. This has greatly simplified the jFEX architecture, increased the dynamic range of the
226 calorimeter data received by L1Calo, and simplified the link protocol, all of which improve
227 L1Calo trigger performance.

228 4. Conclusion

229 The ATLAS Level-1 Calorimeter Trigger will be upgraded as part of the ATLAS Phase-I
230 upgrades for 2019. Development of both the eFEX and jFEX are well underway, with
231 prototypes under test or in manufacture. A systematic PCB design method, centred on PCB
232 simulation and validation, has been used in developing these high-speed, high-density and high-
233 power modules. The test results of the first eFEX prototype are very good, as a result of which
234 the baseline for the speed of links into L1Calo has been increased from 6.4 Gb/s to 11.2 Gb/s,
235 simplifying the architecture and improving the performance of the trigger.

236 References

- 237 [1] Lyndon Evans and Philip Bryant, *LHC Machine*, 2008 JINST 3 S08001.
238 <http://iopscience.iop.org/1748-0221/3/08/S08001>
- 239 [2] ATLAS collaboration, *The ATLAS Experiment at the CERN Large Hadron Collider*, 2008 JINST 3
240 S08003. <http://iopscience.iop.org/1748-0221/3/08/S08003>
- 241 [3] ATLAS collaboration, *ATLAS Level-1 Trigger: TDR*, CERN/LHCC/98-14.
242 <http://atlas.web.cern.ch/Atlas/GROUPS/DAQTRIG/TDR/tdr.html>
- 243 [4] ATLAS collaboration, *Technical Design Report for the Phase-I Upgrade of the ATLAS TDAQ*
244 *System*, CERN-LHCC-2013-018. <https://cds.cern.ch/record/1602235/files/ATLAS-TDR-023.pdf>
- 245 [5] R. Achenbach et al, *The ATLAS Level-1 Calorimeter Trigger*, 2008 JINST 3 P03001.
246 <http://iopscience.iop.org/1748-0221/3/03/P03001>
- 247 [6] Weihao Wu et al, The development of the Global Feature Extractor for the LHC Run-3 upgrade of
248 the L1 Calorimeter trigger system, ATL-DAQ-PROC-2016-010.
249 <https://cds.cern.ch/record/2162162/>
- 250 [7] [https://atlas.web.cern.ch/Atlas/GROUPS/PHYSICS/UPGRADE/CERN-LHCC-2013-](https://atlas.web.cern.ch/Atlas/GROUPS/PHYSICS/UPGRADE/CERN-LHCC-2013-018/fig_19.png)
251 [018/fig_19.png](https://atlas.web.cern.ch/Atlas/GROUPS/PHYSICS/UPGRADE/CERN-LHCC-2013-018/fig_19.png)
- 252 [8] [https://atlas.web.cern.ch/Atlas/GROUPS/PHYSICS/UPGRADE/CERN-LHCC-2013-](https://atlas.web.cern.ch/Atlas/GROUPS/PHYSICS/UPGRADE/CERN-LHCC-2013-018/fig_20.png)
253 [018/fig_20.png](https://atlas.web.cern.ch/Atlas/GROUPS/PHYSICS/UPGRADE/CERN-LHCC-2013-018/fig_20.png)
- 254 [9] [https://atlas.web.cern.ch/Atlas/GROUPS/PHYSICS/UPGRADE/CERN-LHCC-2013-](https://atlas.web.cern.ch/Atlas/GROUPS/PHYSICS/UPGRADE/CERN-LHCC-2013-017/fig_11.png)
255 [017/fig_11.png](https://atlas.web.cern.ch/Atlas/GROUPS/PHYSICS/UPGRADE/CERN-LHCC-2013-017/fig_11.png)
- 256 [10] [https://atlas.web.cern.ch/Atlas/GROUPS/PHYSICS/UPGRADE/CERN-LHCC-2013-](https://atlas.web.cern.ch/Atlas/GROUPS/PHYSICS/UPGRADE/CERN-LHCC-2013-017/fig_14b.png)
257 [017/fig_14b.png](https://atlas.web.cern.ch/Atlas/GROUPS/PHYSICS/UPGRADE/CERN-LHCC-2013-017/fig_14b.png)
- 258 [11] [https://atlas.web.cern.ch/Atlas/GROUPS/PHYSICS/UPGRADE/CERN-LHCC-2013-](https://atlas.web.cern.ch/Atlas/GROUPS/PHYSICS/UPGRADE/CERN-LHCC-2013-018/fig_26.png)
259 [018/fig_26.png](https://atlas.web.cern.ch/Atlas/GROUPS/PHYSICS/UPGRADE/CERN-LHCC-2013-018/fig_26.png)

- 260 [12] AdvancedTCA PCIMG 3.0 Short Form Specification
261 http://www.picmg.org/pdf/PICMG_3_0_Shortform.pdf
- 262 [13] <https://www.xilinx.com/products/silicon-devices/fpga.html>
- 263 [14] MicroPOD™ and MiniPOD™ 120G Transmitters/Receivers
264 http://www.avagotech.com/pages/minipod_micropod
- 265 [15] <http://www.onsemi.com/PowerSolutions/product.do?id=NB7VQ14M>
- 266 [16] W. Qian, *ATLAS level-1 calorimeter trigger upgrade for phase-I, 2013 JINST 8 C01039.*
267 <http://iopscience.iop.org/article/10.1088/1748-0221/8/01/C01039>
- 268 [17] <https://www.altera.com/products/fpga/aria-series/aria-10/overview.html>